



You have downloaded a document from
RE-BUŚ
repository of the University of Silesia in Katowice

Title: Isospin effects studied with the CHIMERA detector at 35 Mev/nucleon

Author: R. Płaneta, F. Amorini, A. Anzalone, L. Auditore, V. Baran, I. Berceanu, Andrzej Grzeszczuk, Seweryn Kowalski, Katarzyna Schmidt, Wiktor Zipper i in.

Citation style: Płaneta R., Amorini F., Anzalone A., Auditore L., Baran V., Berceanu I., Grzeszczuk Andrzej, Kowalski Seweryn, Schmidt Katarzyna, Zipper Wiktor i in. (2006). Isospin effects studied with the CHIMERA detector at 35 Mev/nucleon. "Acta Physica Polonica B" (Vol. 37, no. 1 (2006), s. 183-191).



Uznanie autorstwa - Licencja ta pozwala na kopiowanie, zmienianie, rozprowadzanie, przedstawianie i wykonywanie utworu jedynie pod warunkiem oznaczenia autorstwa.



UNIWERSYTET ŚLĄSKI
W KATOWICACH



Biblioteka
Uniwersytetu Śląskiego



Ministerstwo Nauki
i Szkolnictwa Wyższego

ISOSPIN EFFECTS STUDIED WITH
THE CHIMERA DETECTOR AT 35 MeV/NUCLEON*

R. PŁANETA^{g,†}, F. AMORINI^a, A. ANZALONE^a, L. AUDITORE^d, V. BARAN^e
 I. BERCEANU^e, J. Blicharska^f, J. BRZYCHCZYK^g, B. BORDERIE^h
 R. BOUGAULTⁱ, M. BRUNO^j, G. CARDELLA^b, S. CAVALLARO^a
 M.B. CHATTERJEE^k, A. CHBIH^l, M. COLONNA^a, M. D'AGOSTINO^j
 E. DEFILIPPO^b, R. DAYRAS^o, M. DITORO^a, J. FRANKLAND^l, E. GALICHET^h
 W. GAWLIKOWICZ^u, E. GERACI^j, F. GIUSTOLISI^a, A. GRZESZCZUK^f
 P. GUAZZONI^p, D. GUINET^q, M. IACONO-MANNO^a, S. KOWALSKI^f
 E. LAGUIDARA^a, G. LANZANO^b, G. LANZALONE^a, J. ŁUKASIK^m
 C. MAIOLINO^a, Z. MAJKA^g, N. LE NEINDRE^h, N.G. NICOLIS^t, A. PAGANO^b
 M. PAPA^b, M. PETROVICI^e, E. PIASECKI^r, S. PIRRONE^b, G. POLITI^b, A. POP^e
 F. PORTO^a, M.F. RIVET^h, E. ROSATO^s, F. RIZZO^a, S. RUSSO^p, P. RUSSOTTO^l
 M. SASSIV^p, K. SCHMIDT^f, K. SIWEK-WILCZYŃSKA^r, I. SKWIRA-CHALOT^r
 A. SOCHOCKA^g, M.L. SPERDUTO^b, L. ŚWIDERSKI^r, A. TRIFIRO^d
 M. TRIMARCHI^d, G. VANNINI^j, G. VERDE^b, M. VIGILANTE^s, J.P. WIELECZKO^l
 J. WILCZYŃSKI^c, L. ZETTA^p, W. ZIPPER^f

^aINFN, Laboratori Nazionali del Sud and Dipartimento di Fisica e Astronomia
 Università di Catania, Italy

^bINFN, Sezione di Catania and Dipartimento di Fisica e Astronomia
 Università di Catania, Italy

^cA. Sołtan Institute for Nuclear Studies, Swierk, Warsaw, Poland

^dINFN, Gruppo Collegato di Messina and Dipartimento di Fisica, Università di Messina, Italy

^eInstitute for Physics and Nuclear Engineering, Bucharest, Romania

^fInstitute of Physics, University of Silesia, Katowice, Poland

^gM. Smoluchowski Institute of Physics, Jagellonian University, Cracow, Poland

^hInstitute de Physique Nucleaire, IN2P3-CNRS, Orsay, France

ⁱLPC, ENSI Caen and Universite de Caen, France

^jINFN, Sezione di Bologna and Dipartimento di Fisica, Università di Bologna, Italy

^kSaha Institute of Nuclear Physics, Kolkata, India

^lGANIL, CEA, IN2P3-CNRS, Caen, France

^mH. Niewodniczanski Institute of Nuclear Physics, Cracow, Poland

^oDAPNIA / SPhN, CEA-Saclay, France

^pINFN, Sezione di Milano and Dipartimento di Fisica, Università di Milano, Italy

^qIPN, IN2P3-CNRS and Universite Claude Bernard, Lyon, France

^rInstitute for Experimental Physics, Warsaw University, Warsaw, Poland

^sINFN, Sezione Napoli and Dipartimento di Fisica, Università di Napoli, Italy

^tDepartment of Physics, The University of Ioannina, Ioannina, Greece

^uHeavy-Ion Laboratory, Warsaw University, Warsaw, Poland

(Received November 15, 2005)

* Presented at the XXIX Mazurian Lakes Conference on Physics
 August 30–September 6, 2005, Piaski, Poland.

† Corresponding author: ufplanet@cyf-kr.edu.pl

The yield of light charged particles and intermediate mass fragments is studied for the neutron-rich, $^{124}\text{Sn}+^{64}\text{Ni}$, and neutron-poor, $^{112}\text{Sn}+^{58}\text{Ni}$, reactions at 35 MeV/nucleon as a function of the impact parameter. Our main observations are: (i) The yields of ^1H , ^3He and ^4He particles in the neutron-poor system are enhanced with respect to the neutron-rich system and the yield of ^3H is suppressed at all impact parameters, (ii) The ratio of ^3H to ^3He yield is three times larger for neutron poor system, (iii) The N/Z ratio of the emitted intermediate-mass fragments shows dependence on the isospin of the system, (iv) The neutron richness of detected intermediate mass fragments depends strongly on their rapidity. The gross features of the experimental data are reproduced by quantum molecular dynamics model calculations.

PACS numbers: 25.70.Mn, 25.70.Pq

1. Introduction

The isospin dependence of nuclear equation of state, NEOS, is among the most important but poorly known properties of nuclear matter [1–3]. The knowledge of the density dependence of the symmetry energy term in NEOS is important for: (i) nuclear structure studies [4, 5], (ii) nuclear reaction models, and (iii) the mechanism of nuclear multifragmentation. The interest in the properties of neutron rich nuclear matter has also an astrophysical aspect, namely, the mechanism of type II supernova explosions, and the formation and structure of neutron stars.

Several experimental observables have been proposed to obtain information on the symmetry energy term, $E_{\text{sym}}(\rho)$, of the NEOS. For the case of low densities of nuclear matter they include measurements of: (i) n/p ratio of fast pre-equilibrium nucleons [6], (ii) $^3\text{H}/^3\text{He}$ ratios, (iii) isospin diffusion [7, 8], (iv) isospin fractionation (distillation) and isoscaling in nuclear multifragmentation [9], (v) neutron–proton differential flow [10], and (vi) neutron–proton and proton–proton correlation functions at low relative momenta [11].

Simulations of reaction dynamics have shown [12], that collisions of asymmetric nuclei (in N/Z) could provide a unique information on the symmetry energy term of NEOS. It was shown that the main reaction mechanisms, from fusion to deep inelastic and fragmentation, appear quite sensitive to the density dependence of the symmetry term in the NEOS. The calculations of Baran *et al.* [3] provide with evidence for characteristic patterns in the behavior of the intermediate mass fragment (IMF) N/Z ratios as a function of the reaction centrality. For peripheral collisions the IMF will be emitted in a statistical way from the excited projectile-like fragment (PLF) and target-like fragment (TLF) sources close to the stability line. For semi-peripheral

events the neck-fragmentation mechanism will form more neutron-rich fragments. For central collisions the neutron distillation will take place and the fragments will again be much more symmetric in N/Z . The relevance of such a behavior is related to the stiffness of the symmetry term at subnuclear densities.

For a class of semi-peripheral collisions the model calculations of the neutron-rich fragment production in the neck region are supported by the experimental results [13–15].

Isoscaling analyses in the peripheral isospin asymmetric collisions for $^{112}\text{Sn} + ^{124}\text{Sn}$, $^{124}\text{Sn} + ^{112}\text{Sn}$ systems at 50 MeV/nucleon imply that the quasiprojectile and quasitarget do not achieve isospin equilibrium, permitting an assessment of isospin transport rates [7]. The BUU transport model simulations predict the isospin diffusion reflecting driving forces arising from the asymmetry term of the NEOS [7]. The novel transport model calculations with the IBUU04 code have shown that the degree of isospin diffusion in heavy-ion collisions at intermediate energies is affected by both the stiffness of the nuclear symmetry energy and the momentum dependence of the nuclear potential [8].

A study of central collision events for the $^{112}\text{Sn} + ^{124}\text{Sn}$, $^{124}\text{Sn} + ^{112}\text{Sn}$, $^{112}\text{Sn} + ^{112}\text{Sn}$, and $^{124}\text{Sn} + ^{124}\text{Sn}$ systems at 50 MeV/nucleon [16] supply the following characteristics of these reactions: *(i)* The gas phase is more enriched in neutrons than the liquid phase represented by fragments. The observation is consistent with the predicted partial fractionation (distillation) of nucleon components in the liquid-gas phase transition, *(ii)* The observed effects are significantly enhanced in neutron-rich systems relative to the neutron-deficient systems. The similar conclusions have been drawn from the analysis for central collisions of $^{124}\text{Sn} + ^{64}\text{Ni}$ and $^{112}\text{Sn} + ^{58}\text{Ni}$ at 35 MeV/nucleon [17]. The isoscaling analysis using the ratios of the isotopic yields has been performed. The results are consistent with the effect of isospin distillation.

In this contribution, we focus our attention to non-central collisions of $^{124}\text{Sn} + ^{64}\text{Ni}$ and $^{112}\text{Sn} + ^{58}\text{Ni}$ systems at 35 MeV/nucleon. The reverse kinematics of studied reactions and the high granularity of the forward part of the CHIMERA detector [18] make possible the detection of particles and fragments originating from the PLF, TLF and intermediate velocity (IVS) sources.

Sec. 2 gives a short information on the REVERSE experiment. The procedure applied for the impact parameter events selection is presented in Sec. 3. The analyses results are discussed in Sec. 4 and the conclusions are presented in Sec. 5.

2. The experimental procedure and the data analysis

The experiment was performed at the LNS in Catania using the forward part of the CHIMERA 4π multidetector array [18]. There were a total of 688 Si-CsI(Tl) detectors used, covering the polar angle range between 1° and 30° with full azimuthal symmetry around the beam axis. Reverse kinematics of $^{124,112}\text{Sn} + ^{64,58}\text{Ni}$ reactions at 35 MeV/nucleon allowed the use of this set-up as an effective 4π device.

In order to identify the reaction products, several identification methods have been used [19]. The mass of the fragments stopped in the silicon detectors was extracted by using the time of flight technique (TOF). The $\Delta E - E$ technique was applied to identify the charge of particles that punch through the silicon detectors and isotopic identification was achieved for fragments with charge up to 9. The light charged particles (LCP) that lose only a small part of their energy in silicon and are stopped in the CsI(Tl) detector were identified applying the pulse shape discrimination method using the signal from a $20\text{ mm} \times 20\text{ mm}$ photodiode, optically coupled to the crystal.

Due to the very good performance of the detectors, identification of atomic numbers up to $Z = 50$ was achieved with a resolution better than unity in the full dynamical range of the experiment. For charged-particles up to $Z = 30$, the TOF technique was used for mass identification. Further details of particle identification and energy calibration can be found in [19].

3. Selection of non-central collisions

In intermediate-energy heavy-ion collisions, the reaction cross-section is dominated by dissipative binary reactions involving well defined projectile- and target-like fragments [20], similar to what is observed at low bombarding energies [21]. Since peripheral collisions represent the bulk of the reaction cross section, their properties characterize the gross features of the reaction. In the following, we concentrate our analysis on non-central collisions (NCC). By the NCC we understand collisions in which the PLF and the TLF are present. Such a definition covers a wide range of impact parameters and does not exclude the existence of the IVS [22–24].

The class of events corresponding to the NCC is selected using conditions: *(i)* the large amount of total charge and projectile momentum are collected in the detected fragments and particles, and *(ii)* the PLF remnant is observed. In the following, our analysis is restricted to the class of well defined events selected by the above conditions.

A comparison between the experimental charge distributions and the QMD/GEMINI [25] [26] predictions for both investigated systems is presented in Fig. 1. Simulated reaction events were selected using the same

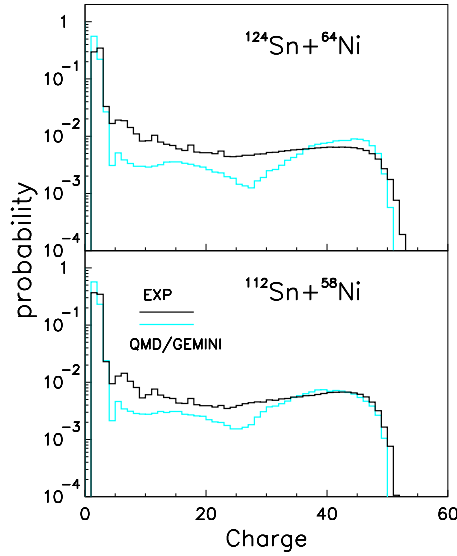


Fig. 1. Charge distributions for $^{124}\text{Sn}+^{64}\text{Ni}$ and $^{112}\text{Sn}+^{58}\text{Ni}$ systems (data — black histograms, calculations — gray histograms).

conditions as the experimental data. As can be seen, the model overestimates the multiplicity of light particles and at the same time underestimates the IMF emission.

In order to study the evolution of heavy-ion reactions with respect to the centrality of the collision it is necessary to use impact parameter related variables. Such variables allow us to analyze the reaction evolution with respect to excitation energy, energy dissipation, entrance channel angular

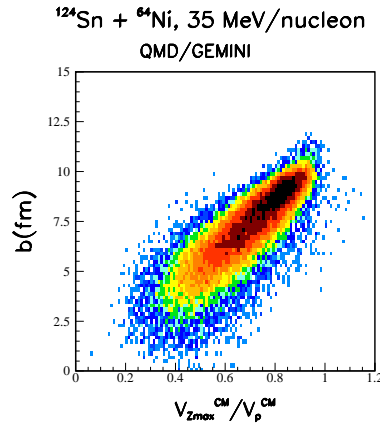


Fig. 2. Impact parameter estimator for $^{124}\text{Sn}+^{64}\text{Ni}$ reaction at 35 MeV/nucleon.

momentum, *etc.* [27]. We have tested several variables as impact parameter estimators, using the QMD/GEMINI model calculations for the class of the NCCs. Fig. 2 shows a correlation between impact parameter b , and velocity of the heaviest fragment in units of the projectile velocity in the CM system, $V_{Z_{\max}}^{\text{CM}}/V_p^{\text{CM}}$. The results presented in this paper are for the $V_{Z_{\max}}^{\text{CM}}/V_p^{\text{CM}}$ estimator where the best sensitivity to the impact parameter is observed.

4. Impact parameter dependence of isospin effects

The Fig. 3 shows the yield of different isotopes per event as a function of impact parameter estimator $V_{Z_{\max}}^{\text{CM}}/V_p^{\text{CM}}$ for both studied systems. As expected the multiplicity of the LCP emission increases with the centrality of the collision. Important observation is that the ${}^3\text{He}$ yield is higher for the neutron poor system in contrast to the ${}^3\text{H}$ which are emitted more abundantly from the neutron rich system.

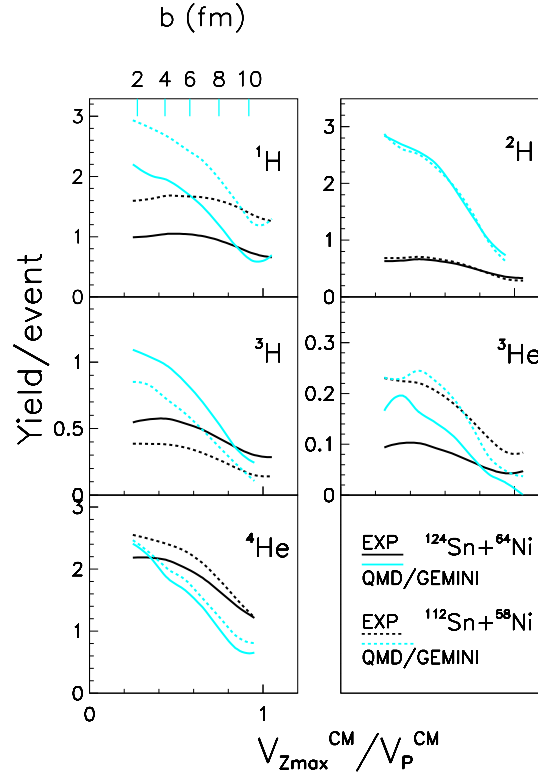


Fig. 3. Yield per event of light particles as a function of velocity of the heaviest fragment normalized to the projectile velocity $V_{Z_{\max}}^{\text{CM}}/V_p^{\text{CM}}$ for the ${}^{124}\text{Sn}+{}^{64}\text{Ni}$ and ${}^{112}\text{Sn}+{}^{58}\text{Ni}$ systems. An estimate of the impact parameter is shown on the top.

The predictions of the QMD/GEMINI simulations are close to experimentally observed yields for very peripheral collisions (large $V_{Z_{\max}}^{\text{CM}}/V_p^{\text{CM}}$). With an increase of collision centrality (decrease of $V_{Z_{\max}}^{\text{CM}}/V_p^{\text{CM}}$) the model overestimates the emission rates, especially for hydrogen isotopes.

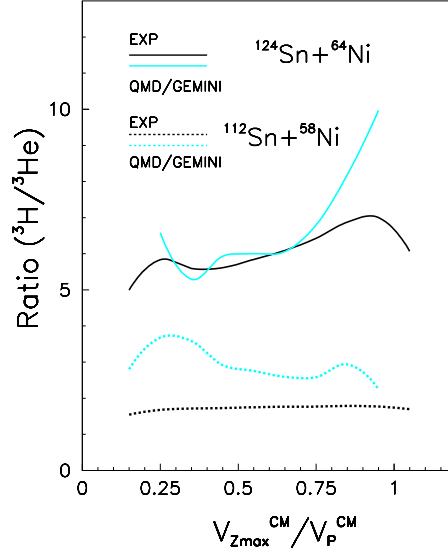


Fig. 4. Ratio of ${}^3\text{H}$ to ${}^3\text{He}$ yield as a function of $V_{Z_{\max}}^{\text{CM}}/V_p^{\text{CM}}$ for the ${}^{124}\text{Sn}+{}^{64}\text{Ni}$ and ${}^{112}\text{Sn}+{}^{58}\text{Ni}$ systems.

The influence of the entrance channel on the particle production can be seen in Fig. 4 where the ratio of tritons to ${}^3\text{He}$ yield per event is shown. One observes that for the neutron-rich system the number of tritons is about six times larger than the number of ${}^3\text{He}$ particles. For the neutron-poor system this ratio is much lower, at the level of 1.5.

Inspection of velocity spectra of IMFs shows that heavier IMF's are preferentially located close to the midrapidity region. The number of fragments observed in the PLF region is strongly reduced. To get more information about the mechanism of the IMF production for both systems we have plotted in Fig. 5 the average N/Z ratio for IMFs as a function of parallel velocity of the fragment in the CM system. Different curves correspond to different centrality regions selected by the impact parameter estimator $V_{Z_{\max}}^{\text{CM}}/V_p^{\text{CM}}$. One can observe a significant evolution of the N/Z ratio as a function of parallel velocity. Fragments with velocities close to the center of mass velocity are more neutron rich than the fragments located in the PLF region. One can also see that the curves for the neutron-rich system are located higher than the curves corresponding to the neutron-poor system.

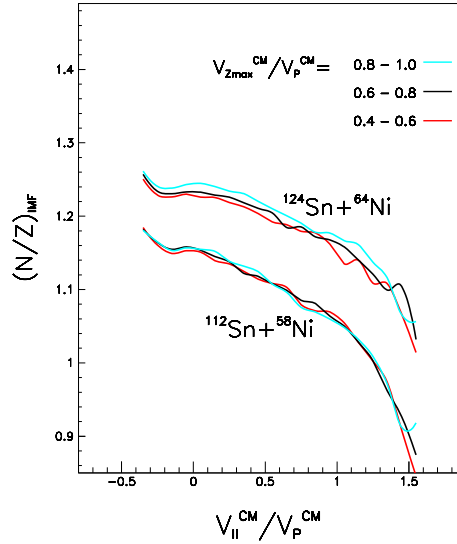


Fig. 5. The average N/Z ratio of IMFs ($Z_{\text{IMF}} = 4 - 8$) for the $^{124}\text{Sn}+^{64}\text{Ni}$ and $^{112}\text{Sn}+^{58}\text{Ni}$ reactions as function of parallel velocity of the fragment normalized to the projectile velocity, $V_{\parallel}^{\text{CM}}/V_p^{\text{CM}}$. Different curves correspond to different windows of $V_{Z_{\text{max}}}^{\text{CM}}/V_p^{\text{CM}}$.

5. Conclusions

Isospin effects were studied for the neutron-rich $^{124}\text{Sn}+^{58}\text{Ni}$ and neutron-poor $^{124}\text{Sn}+^{64}\text{Ni}$ reactions at 35 MeV/nucleon. Our main observations are: (i) In both systems the number of emitted alpha particles is greater than the number of protons. This effect is more pronounced in the neutron-rich system and increases with the centrality of the collision. (ii) The ratio of ^3H to ^3He is about 3 times higher in the neutron-rich system and its impact parameter dependence is relatively weak. (iii) In both reactions the neutron richness of the observed fragments increases with the fragment's decreasing velocity in the range from that of PLF's to the midrapidity region.

There is a qualitative agreement between our experimental findings and QMD calculations performed with a stiff parametrization of the symmetry energy strength of NEOS.

This work was partly supported by the Polish State Committee for Scientific Research (KBN) grant No. 2P03B11023. One of the authors (N.G.N.) acknowledges the financial support from the cross-cultural programme between the Ministries of Education of Poland and Greece for the year 2005.

REFERENCES

- [1] Bao-An Li *et al.*, *Int. J. Mod. Phys.* **E7**, 147 (1998).
- [2] Bao-An Li *et al.*, *Nucl. Phys.* **A699**, 493 (2002).
- [3] V. Baran *et al.*, *Nucl. Phys.* **A703**, 603 (2002).
- [4] B. Alex Brown, *Phys. Rev. Lett.* **85**, 5296 (2000).
- [5] C.J. Horowitz, J. Piekarewicz, *Phys. Rev. Lett.* **86**, 5647 (2001).
- [6] W.U. Schröder, J. Töke, *Nucl. Phys.* **A681**, 418c (2001).
- [7] M.B. Tsang *et al.*, *Phys. Rev. Lett.* **92**, 062701 (2004).
- [8] Lie-Wen Chen *et al.*, *Phys. Rev. Lett.* **94**, 032701 (2005).
- [9] A. Ono *et al.*, *Phys. Rev.* **C68**, 051601 (2003).
- [10] Bao-An Li, *Phys. Rev. Lett.* **85**, 4221 (2000).
- [11] R. Ghetti *et al.*, *Phys. Rev.* **C69**, 031605 (2004).
- [12] M. Colonna *et al.*, *Phys. Rev.* **C57**, 1410 (1998).
- [13] E. Plagnol *et al.*, *Phys. Rev.* **C61**, 014606 (2000).
- [14] P.M. Milazzo *et al.*, *Nucl. Phys.* **A703**, 466 (2002).
- [15] S. Hudan *et al.*, *Phys. Rev.* **C71**, 054604 (2005).
- [16] H.S. Xu *et al.*, *Phys. Rev. Lett.* **85**, 716 (2000).
- [17] E. Geraci *et al.*, *Nucl. Phys.* **A732**, 173 (2004); E. Geraci *et al.*, *Nucl. Phys.* **A734**, 524 (2004).
- [18] A. Pagano *et al.*, *Nucl. Phys.* **A681**, 331 (2001) and references therein.
- [19] M. Alderighi *et al.*, INFN-LNS Activity Report 2000, p. 59; J. Blicharska *et al.*, INFN-LNS Activity Report 2001, p. 113; N. Le Neindre *et al.*, *Nucl. Instrum. Methods* **A490**, 251 (2002); M. Alderighi *et al.*, *Nucl. Instrum. Methods* **A489**, 257 (2002).
- [20] S.P. Baldwin *et al.*, *Phys. Rev. Lett.* **74**, 1299 (1995).
- [21] See for example: W.U. Schröder, J.R. Huizenga, *Treatise on Heavy-Ion Science*, Plenum Press, New York and London 1984, Vol. 2, p. 113–726.
- [22] J. Töke *et al.*, *Nucl. Phys.* **A583**, 519 (1995); *Phys. Rev. Lett.* **77**, 3514 (1996).
- [23] L. Stuttgè *et al.*, *Nucl. Phys.* **A539**, 511 (1992).
- [24] L.G. Sobotka, *et al.*, *Phys. Rev.* **C62**, 031603(R) (2000).
- [25] J. Łukasik, Z. Majka, *Acta Phys. Pol. B* **24**, 1993 (1993); J. Łukasik, Ph.D. Thesis, Kraków 1993.
- [26] J. Aichelin, H. Stöcker, *Phys. Lett.* **B176**, 14 (1986); J. Aichelin, *Phys. Rep.* **202**, 233 (1991).
- [27] J.D. Frankland *et al.*, *Nucl. Phys.* **A689**, 905 (2001).